

RESEARCH ARTICLE

Endogenous cerebellar neurogenesis in adult mice with progressive ataxia

Manoj Kumar^{1,2}, Zsolt Csaba^{1,2}, Stéphane Peineau^{1,2,3}, Rupali Srivastava^{1,2,4}, Sowmyalakshmi Rasika^{1,2}, Shyamala Mani⁵, Pierre Gressens^{1,2,6} & Vincent El Ghouzzi^{1,2}

¹Inserm U1141, Paris, France

²Sorbonne Paris Cité, Université Paris Diderot, UMRS 1141, Paris, France

³School of Physiology and Pharmacology, MRC Centre for Synaptic Plasticity, Bristol, United Kingdom

⁴National Brain Research Centre, Manesar, India

⁵Centre for Neuroscience, IISC, Bangalore, India

⁶Department of Division of Imaging Sciences and Biomedical Engineering, Centre for the Developing Brain, King's College London, King's Health Partners, St. Thomas' Hospital, London, United Kingdom

Correspondence

Vincent El Ghouzzi, Inserm U1141, Hôpital Robert-Debré, 48 Boulevard Sérurier, F-75019 Paris, France. Tel: +331 40031973; Fax: +331 40031995; E-mail: vincent.elghouzzi@inserm.fr

Funding Information

This study was supported by the Institut National pour la Santé et la Recherche Médicale (Inserm), the Centre National de la Recherche Scientifique (CNRS), the Université Paris7, the DHU PROTECT and grants from IFCPAR/CEFIPRA (project nos. 3803-3 and 4903-2), the French National Research Agency (project ANR-09-GENO-007), the Princesse Grâce de Monaco Foundation and the Roger de Spoelberch Foundation. M. K. was supported by the Inserm and ANR contract no. ANR-09-GENO-007 to V. E. G.

Received: 8 October 2014; Accepted: 10 October 2014

Annals of Clinical and Translational Neurology 2014; 1(12): 968–981

doi: 10.1002/acn3.137

Introduction

Inherited cerebellar ataxias, a heterogeneous group of neurodegenerative disorders characterized by progressive degeneration and resulting in impaired balance, gait, and movement coordination,¹ are a major cause of disability and reduced life-span, with few treatment options. The Harlequin (Hq) mouse is a spontaneous genetic mouse

Abstract

Objective: Transplanting exogenous neuronal progenitors to replace damaged neurons in the adult brain following injury or neurodegenerative disorders and achieve functional amelioration is a realistic goal. However, studies so far have rarely taken into consideration the preexisting inflammation triggered by the disease process that could hamper the effectiveness of transplanted cells. Here, we examined the fate and long-term consequences of human cerebellar granule neuron precursors (GNP) transplanted into the cerebellum of Harlequin mice, an adult model of progressive cerebellar degeneration with early-onset microgliosis. **Methods:** Human embryonic stem cell-derived progenitors expressing Atoh1, a transcription factor key to GNP specification, were generated in vitro and stereotaxically transplanted into the cerebellum of preataxic Harlequin mice. The histological and functional impact of these transplants was followed using immunolabeling and Rotarod analysis. **Results:** Although transplanted GNPs did not survive beyond a few weeks, they triggered the proliferation of endogenous nestin-positive precursors in the leptomeninges that crossed the molecular layer and differentiated into mature neurons. These phenomena were accompanied by the preservation of the granule and Purkinje cell layers and delayed ataxic changes. In vitro neurosphere generation confirmed the enhanced neurogenic potential of the cerebellar leptomeninges of Harlequin mice transplanted with exogenous GNPs. **Interpretation:** The cerebellar leptomeninges of adult mice contain an endogenous neurogenic niche that can be stimulated to yield mature neurons from an as-yet unidentified population of progenitors. The transplantation of human GNPs not only stimulates this neurogenesis, but, despite the potentially hostile environment, leads to neuroprotection and functional amelioration.

model of cerebellar ataxia with an 80–90% reduction in the mitochondrial protein Apoptosis-inducing factor,² which leads to progressive ataxia with selective cerebellar granule neuron loss and subsequently, Purkinje cell death.² Although the first signs of ataxia begin at 4–5 months of age, the degenerative process is already underway by 2 months, with visible signs of mitochondrial degeneration in both granule and Purkinje neurons,

accompanied by widespread inflammatory changes including astrogliosis and microgliosis.³ Thus, the type and temporal characteristics of the neuronal loss observed as well as the combination of inflammatory and neurodegenerative changes make the Hq mouse eminently suitable for the study of such cerebellar ataxias, and cell-replacement strategies aimed at treating them.

The capacity of embryonic stem cells (ESCs) to self-propagate *in vitro* and differentiate into functional neurons in response to extrinsic cues has raised the hope that neurodegenerative diseases in which specific subtypes of neurons progressively degenerate could be treated by stem cell-based replacement strategies. In the present study, we asked whether human ESC-derived granule neuron precursors (GNPs) generated *in vitro* could survive *in vivo* and induce histological and functional improvements in the Hq mouse. Surprisingly, GNPs transplanted into the cerebellum of preataxic Hq mice reduced neurodegenerative changes, slowed the progression of ataxia, and stimulated endogenous neurogenesis from a previously unsuspected niche in the cerebellar leptomeninges.

Materials and Methods

Animals and ethics statement

B6CBACaAw-J/A-Pdc8Hq/J mice (Jackson Laboratory, Bar Harbor, Maine, USA) were housed under a 12 h light/dark cycle with food and water *ad libitum*, and care taken to ensure that ataxic animals could access food and water despite their weakness. Animal procedures were designed to minimize suffering, approved by the Debré-Bichat National Ethics Committee (Project No. 2010-13/676-0018) and conformed to French laws on animal protection.

Generation of Atoh1-driven NLS-GFP-expressing cells from undifferentiated hESCs

The human HUES-4 and HUES-7 lines from Harvard were used at passages 35–55, and verified for normal karyotype and pluripotency. For Atoh1-driven NLS-GFP (green fluorescent protein)-expressing cell line generation, cells were stably transfected with the pJ2XnGFP-Hygro plasmid derived from pJ2XnGFP, kindly provided by Prof. Johnson (Dallas, TX⁴). Briefly, pJ2XnGFP was modified by the introduction of the hygromycin gene between the Kpn1 and Xho1 restriction sites, linearized and transfected using Lipofectamine 2000 (*Life Technologies*, Saint Aubin, France) under feeder-free conditions. Hygromycin-resistant clones were generated and used for neuronal differentiation.

Differentiation of hESCs into GNPs and mature granule neurons

Cells were grown in six-well plates on inactivated mouse embryonic fibroblasts (iMEFs) with daily changes of hESC medium (Knockout-DMEM, 20% Knockout-SR, 1× penicillin-streptomycin, 1× NEAA, 1× GlutaMax, 1× β -mercaptoethanol, 10 ng/mL bFGF [all from *Life Technologies*]). For neural induction, hESCs were seeded onto low-adherence plates to allow embryoid body (EB) formation. EBs were grown in hESC medium without bFGF for 8 days and 10 μ mol/L retinoic acid (Sigma-Aldrich, St. Louis, MO, USA) was added on days 4 and 6. On day 8, EBs were cultured on Matrigel-coated plates for 6–10 days in DMEM/F12 with 200 mmol/L glutamine, antibiotics, 20 ng/mL bFGF, 1× Insulin-Transferrin-Selenium (*Life Technologies*). After 6–10 days, neurospheres (NS) were manually isolated, plated on coated Petri plates and cultured in DMEM/F12 with 1× N2, 1× B27, 100 ng/mL FGF8, 50 ng/mL Wnt3a, 20 ng/mL BMP6, 100 ng/mL BMP7, and 100 ng/mL GDF7 (all from R&D Systems, Minneapolis, MN, USA) for the first 4 days (NS+4) with the addition of 100 ng/mL Shh for another 4 days (NS+8). Cells were then treated with 0.025% Trypsin/EDTA at 37°C for 2–3 min to make single cell suspensions. For final differentiation (FD), 10⁵ cells were grown on coated coverslips in 24-well plates in Neurobasal medium containing 1× N2, 1× B27, 100 ng/mL FGF8, 50 ng/mL Wnt1, 50 ng/mL Wnt3a, 20 ng/mL BMP6, 100 ng/mL BMP7, 100 ng/mL GDF7, 100 ng/mL Shh, and 20 ng/mL Jag1. The medium was changed every alternate day.

RNA extraction and quantification of relative gene expression by real-time PCR

Total RNA was extracted from cells at NS+4, NS+8, and FD+7 stages using an RNA extraction Kit (Qiagen, Courtaboeuf, France) and used to synthesize cDNA (Bio-Rad, Marnes-la-Coquette, France). Real-time PCRs were performed as previously reported, in triplicate with negative and internal (HPRT) controls.⁵ Primers for quantitative real-time PCR are given in Table 1.

Cell transplantation and immunofluorescence

Twenty-four hours before transplantation, mice were injected intraperitoneally with 10 mg/kg ciclosporin (Novartis, Basel, Switzerland). Stereotaxic injections of GNPs into the cerebellum were carried out as previously described.⁵ Following injection, Alzet pumps (DURECT, Cupertino, CA, USA) filled with ciclosporin (10 mg/kg per day) were transplanted subcutaneously

Table 1. Primers and annealing temperatures used for real-time PCR.

Primer	Sequence forward/reverse (5'-3')	Amplicon size (bp)	Annealing temp (°C)
Pax6	AGGTATTACGAGACTGGCTCC/TCCCGCTTACTGGGCTATTT	104	60
Atoh1	GAGTGGGCTGAGGTAAGAGT/GGTCGGTGCTATCCAGGAG	151	60
Zic1	CAGTATCCCGCGATTGGTGT/GCGAACTGGGGTTGAGCTT	139	60
Zic2	CCGTCCAGTGTGAGTTTGAG/CTTGCAGAGATAGGGCTTATCG	105	60
Hprt	GGTAAAAGGACCCACGA/TCAAGGGCATATCCTACAACA	261	60

and replaced monthly. Procedures for sample preparation and immunolabeling were performed as described.⁵ All antibodies and concentrations used are listed in Table 2. For BrdU incorporation, mice received BrdU intraperitoneally (50 mg/kg) every alternate day for 30 days, starting at 5 months, and sacrificed at 7 months. After antigen retrieval, sections were treated with 2 mol/L HCl for 30 min followed by 0.1 mol/L Sodium Borate for 5 min, and normal labeling performed.

Table 2. List of primary and secondary antibodies used for immunofluorescence.

Antibody	Company	Catalog	Dilution
Primary			
Laminin	Sigma	L9393	1:2000
Ki67	BD	556003	1:250
MAP2	Abcam	ab11268	1:400
Zic1	Abcam	ab72694	1:200
Zic2	Abcam	ab12072	1:200
hNestin	Millipore	MAB5326	1:200
mNestin	Millipore	MAB353	1:200
AHN	Millipore	MAB1281	1:200
Tuj1	Covance	435P-0250	1:1000
Atoh1 (Math1)	Abcam	ab22270	1:200
Pax6	Millipore	MAB5552	1:200
NeuN	Millipore	MAB377	1:500
Calbindin 28	Swant	300	1:2000
Iba1	Wako	19-19741	1:1000
CD206	Serotec	MCA2235	1:50
BrdU	BD	347580	1:100
S100	Abcam	ab41548	1:3000
GABA _A R- α 6	Millipore	AB5610	1:1000
MAP2	Millipore	AB5622	1:500
Ki67	Abcam	Ab16667	1:200
SC121	Stemcellsin	STEM121	1:1000
DCX	Abcam	ab18723	1:200
Secondary			
Donkey Anti-Mouse IgG (AF 488)	Life Technologies	A-21202	1:1000
Donkey Anti-Mouse IgG (AF594)	Life Technologies	A-21203	1:1000
Donkey Anti-Rabbit IgG (AF488)	Life Technologies	A-21206	1:1000
Donkey Anti-Rabbit IgG (AF594)	Life Technologies	A-21207	1:1000
Donkey Anti-Rat IgG (AF594)	Life Technologies	A-21209	1:1000

Rotarod assay

Control ($n = 12$) and GNP-treated ($n = 14$) mice were placed on a computer-driven Rotarod device (Imetronic) accelerating linearly from 4 to 40 rpm over a 5-min period, following the protocol initially adapted by Klein for Hq mice.² The latency to fall was averaged from the results of three trials. Data were expressed as a percentage of the initial performance for each animal.

Culture of leptomeninges

Leptomeninges from the cerebellar surface were stripped mechanically, collected in PBS, centrifuged at $500\times g$ and resuspended in Neurobasal medium containing $1\times N2$ -supplement, $1\times B27$, 200 mmol/L glutamine, antibiotics and 10 ng/mL bFGF. On Day 10, the growing leptomeninges were trypsinized into small pieces and plated onto coverslips coated with 100 μ g/mL polyornithine and 10 μ g/mL laminin (Sigma) in Neurobasal medium containing $1\times N2$ supplement, $1\times B27$, 200 mmol/L glutamine, antibiotics and 50 ng/mL BDNF (R&D Systems). Meninges were cultured for an additional 10 days with a change of medium every alternate day.

Electrophysiology

Experiments were performed on differentiated stem cell cultures. Cells were continuously superfused in recording solution consisting of (in mmol/L): NaCl, 124; KCl, 3; NaHCO₃, 26; NaH₂PO₄, 1.25; CaCl₂, 2; MgSO₄, 1; glucose, 10. Visually guided whole-cell recordings were obtained from the soma of neuron-like cells using patch electrodes (4–6 M Ω) that contained in (mmol/L): KCl, 140; HEPES, 10; NaCl, 8; EGTA, 0.5; Mg-ATP, 4; Na-GTP, 0.3. Voltage was recorded on-line using current-clamp techniques. Data were analyzed using the LTP Program.^{6,7}

Results

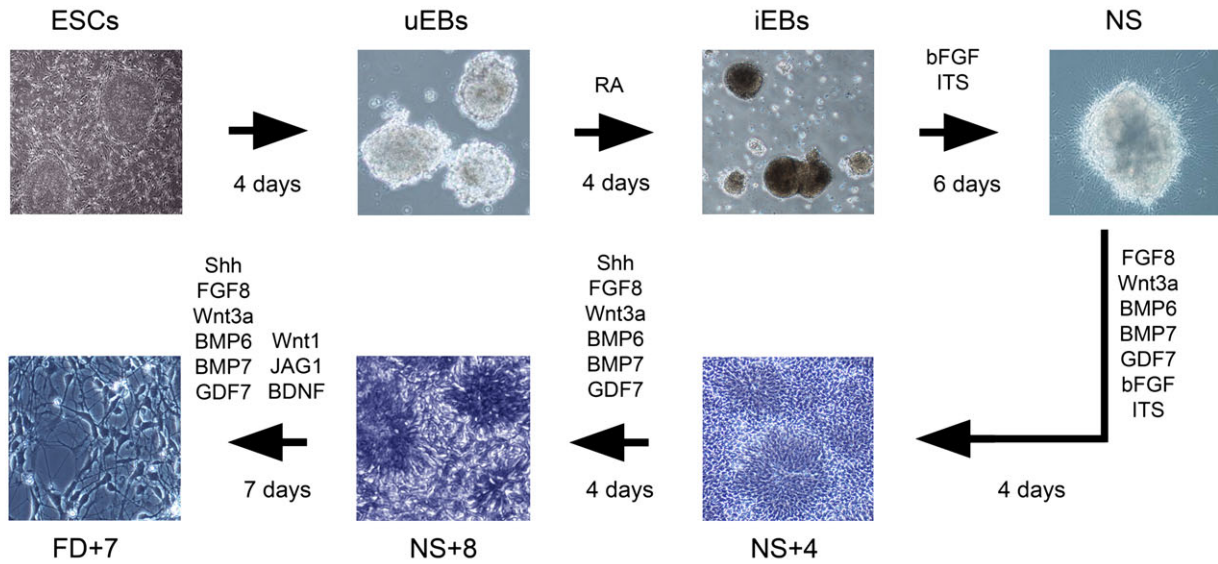
Human GNP generation

Because Atoh1 is key to the control of cerebellar granule cell differentiation,^{5,8} we reasoned that transplanting

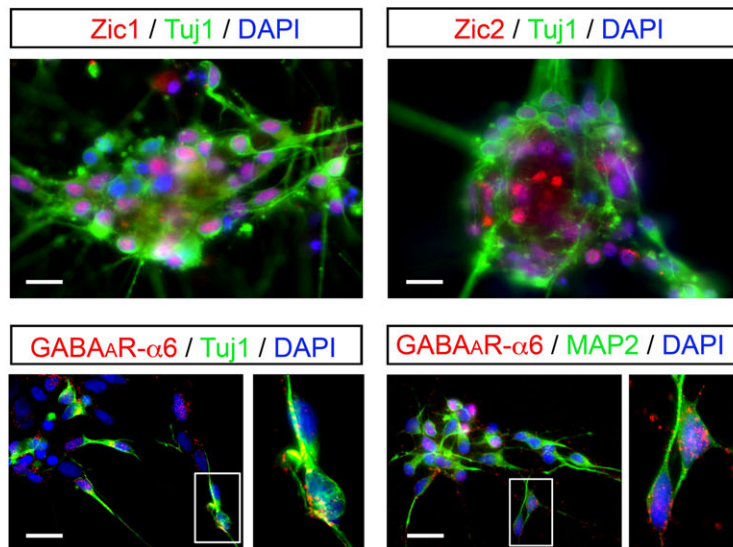
GNPs at a stage when *Atoh1* expression is maximal would enhance our chances of obtaining efficient differentiation *in vivo*. To identify this stage, we generated HUES-4 cells-expressing GFP localized to the nucleus (NLS-GFP) under

the *Atoh1* promoter. ESCs were first induced to differentiate following the sequence of embryoid bodies (EB), proliferative neural stem cells (NS), differentiating GNPs (NS+4 and NS+8), and mature granule neurons (FD+7)

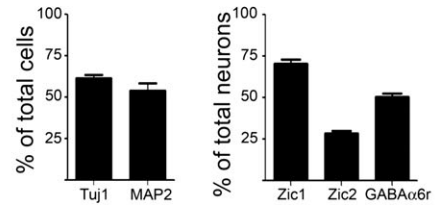
A



B



C



D

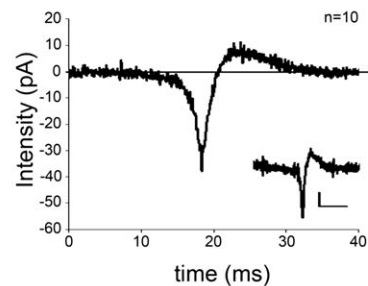


Figure 1. Differentiation of human embryonic stem cells (ESCs) into mature cerebellar granule neurons. (A) Design of the six step-differentiation procedure used to generate mature cerebellar neurons *in vitro*. Undifferentiated cells were grown into embryoid bodies (uEBs) using low-adherence dishes, a neural fate induced with retinoic acid (RA; iEBs), and grown into heterogeneous neurospheres (NS) from which typical neural rosettes developed (NS+4), proliferated (NS+8) and differentiated into neurons (FD+7). (B and C) Immunocytochemistry and cell counts of mature cerebellar granule neurons using early (Tuj1, Zic1, Zic2) and mature neuron-specific markers (MAP2, GABA_AR-α6). Scale bar: 25 μm. (D) Electrophysiological analysis of a mature cerebellar granule neuron at FD+7 showing a spontaneous action potential. Voltage was recorded online using current-clamp techniques. Data were analyzed using the LTP Program.^{6,7}

(Fig. 1A). After 30–40 days in culture, almost all TuJ1-positive cells were also positive for the mature neuronal marker MAP2, indicating that neuronal maturation had been properly achieved (Fig. 1C). In addition, a significant number of neurons expressed markers for cerebellar granule cells such as Zic1 (70.8%), Zic2 (28.3%), and GABA_AR- α 6 (50.6%) (Fig. 1B and C). To examine the functionality of the neurons produced, we performed electrophysiological measurements in vitro. Cells were recorded in current-clamp mode to assess whether they were able to generate an action potential. Spontaneous action potentials were systematically recorded in the long T-shaped processes and ovoid cell bodies typical of granule cells (Fig. 1D). These data indicate that human ESCs can be differentiated into granule neurons capable of generating action potentials in vitro. Next, ESCs were

analyzed for GFP expression. GFP expression was maximal at NS+8 but decreased drastically at FD+7 (Fig. 2A), consistent with 50–65% higher Atoh1 expression at NS+8 than at NS+4 or FD+7 (Fig. 2B). Accordingly, Pax6, a marker of proliferative GNPs, as well as Zic1 and Zic2 were highly expressed at NS+8. These data were confirmed by immunocytochemistry (Fig. 2B and C) and reproduced in a second cell line (HUES-7). We therefore selected the NS+8 stage for subsequent GNP transplantation experiments.

GNP-transplanted Hq mice display better cerebellar preservation

To evaluate the long-term effects of GNP transplantation into the degenerating cerebellum, NS+8 GNPs were

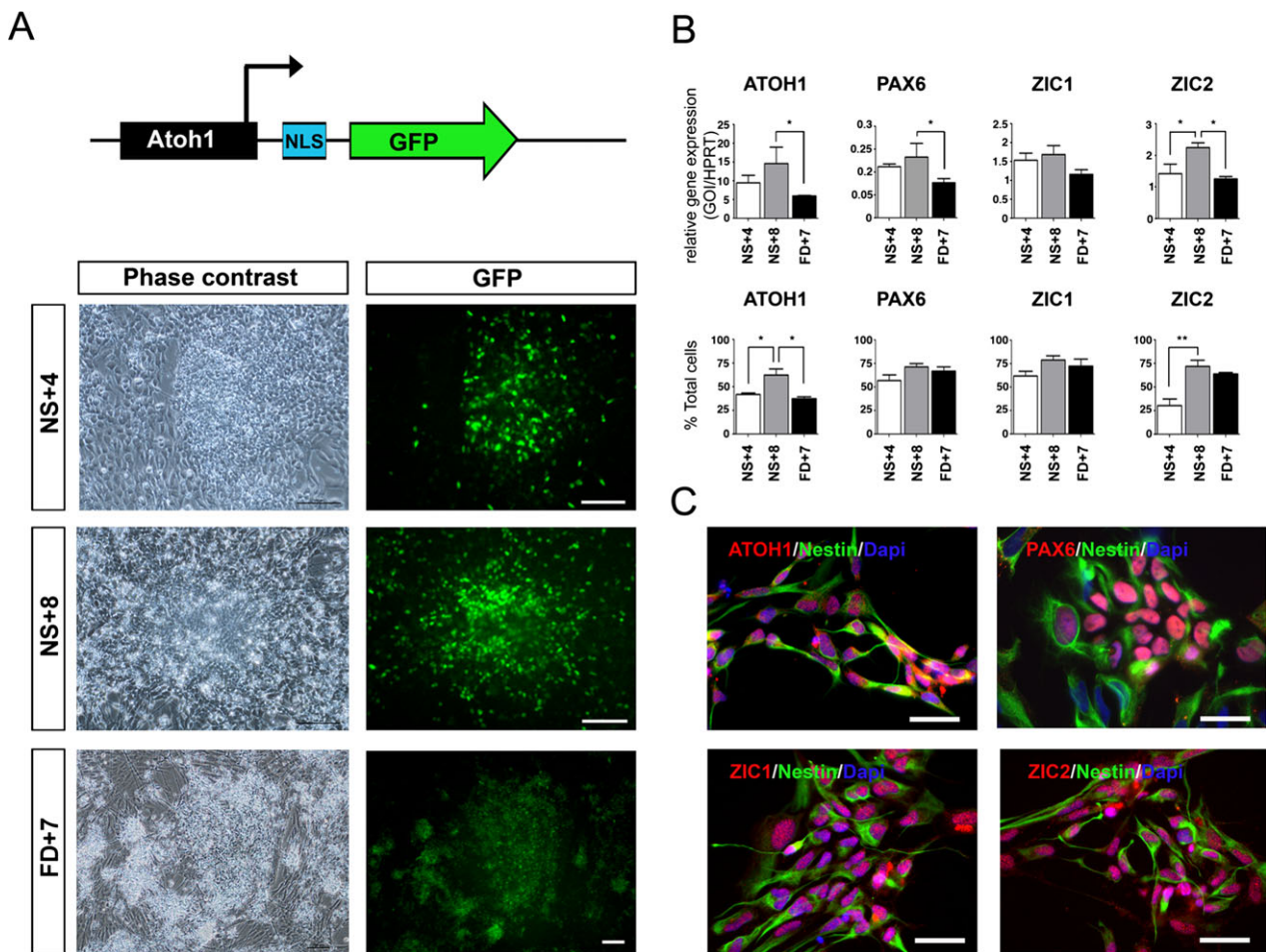


Figure 2. Identification of the stage with maximum Atoh1 expression. (A) An observation of various differentiation stages of a modified HUES-4 line stably expressing green fluorescent protein localized to the nucleus under the control of the Atoh1 promoter shows that NS+8 neurospheres express the highest levels of GFP. Scale bar: 100 μ m. (B) Real-time PCR and cell counting of early transcription factors expressed in GNPs confirm that the NS+8 stage corresponds to the stage at which the highest levels of Atoh1, Pax6, Zic1, and Zic2 are seen. Quantitative data are expressed as means \pm SEM for each group. Results were compared using a one-way ANOVA (GraphPad Prism Software). Significant effects are indicated by asterisks (* P < 0.05, ** P < 0.01). (C) Immunocytochemistry for Atoh1, Pax6, Zic1, and Zic2 in NS+8 neurospheres. Scale bar: 25 μ m.

injected into the cerebellum of 3-month-old preataxic mice and cerebella were analyzed 2 and 4 months after transplantation. Control groups consisted of sham-operated preataxic mice injected with PBS alone. At 2 months post-transplantation, the density of NeuN-positive nuclei in the granule cell layer appeared similar between control and GNP-treated animals, although slightly more nuclei were counted in folia surrounding the transplanted area (folia III–VI) in the GNP-treated group (Fig. 3A). While calbindin labeling showed that most Purkinje cells were still present at this age (Fig. 3B), Fluoro-Jade B labeling revealed that many of these were undergoing degeneration in control animals only, suggesting that Purkinje cells were protected from degeneration in GNP-treated animals (Fig. 4). At 4 months posttransplantation, the number of NeuN-positive nuclei was greatly reduced in the granule cell layer

in the control group, but neuronal density was fairly well preserved in GNP-treated animals, with NeuN-positive cell numbers comparable to those seen 2 months posttransplantation (Fig. 3C). Similarly, in control mice, more than half the Purkinje cells had disappeared 4 months after surgery, while this layer was better preserved in GNP-treated animals (Fig. 3D). Together, these data indicate that GNP transplantation resulted in the significant long-term protection of both granule and Purkinje neurons in Hq mice.

GNP-transplanted Hq mice display improved sensorimotor coordination

To measure sensorimotor coordination in Hq mice, we used the same accelerating rotarod test originally described.² Mice were placed on a rotarod accelerating linearly from 4 to

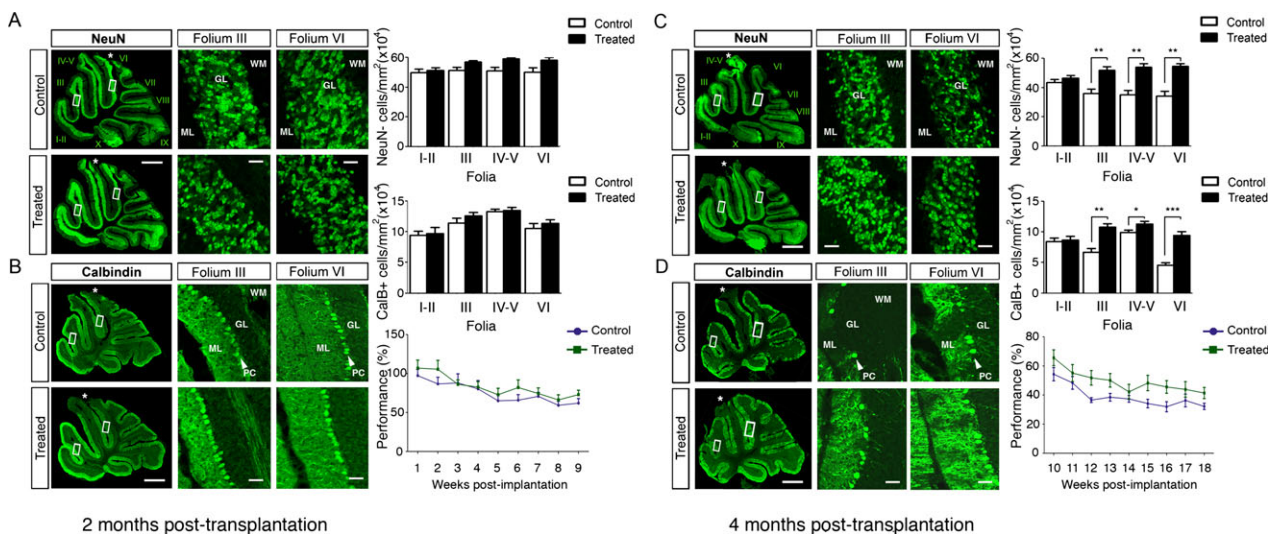


Figure 3. Cerebellar structure and behavioral analysis of GNP-transplanted Hq mice 2 months (8 weeks) and 4 months (16 weeks) posttransplantation. (A) NeuN labeling and cell counts 2 months (8 weeks) after GNP transplantation. Cerebellar folia are numbered and white asterisk indicates the site of injection. White rectangles indicate the area from folia III and VI that are shown in higher magnification. Different cerebellar layers are also indicated: WM (white mater), GL (granule cell layer), ML (molecular layer). No significant difference is seen in the number of granule neurons in the cerebellum of 5-month-old control ($n = 5$) versus GNP-treated Hq mice ($n = 5$). (B) Calbindin-D28k labeling and cell counts 2 months (8 weeks) after GNP transplantation. White asterisk indicates the site of injection. White rectangles indicate the area from folia III and VI that are shown in higher magnification. Different cerebellar layers are also indicated: WM (white mater), GL (granule cell layer), PC (Purkinje cell layer) and ML (molecular layer). No significant difference is seen in the number of Purkinje cells in the cerebellum of 5-month-old control versus GNP-treated Hq mice. Scale bars: 1 mm for whole cerebella and 25 μm for magnifications. Rotarod analysis indicates that motor coordination decreases similarly in the two groups up to this time point. (C) NeuN labeling and cell counts 4 months (16 weeks) after GNP transplantation show that a significantly greater number of granule neurons are protected from death in the GNP-treated group ($n = 5$) as compared to the control group ($n = 6$). Cerebellar folia are numbered and white asterisk indicates the site of injection. White rectangles indicate the area from folia III and VI that are shown in higher magnification. Different cerebellar layers are also indicated: WM (white mater), GL (granule cell layer), ML (molecular layer). (D) Calbindin-D28k labeling and cell counts 4 months (16 weeks) after GNP transplantation show that a significantly greater number of Purkinje cells are protected from death in the GNP-treated group as compared to the control group. White asterisk indicates the site of injection and white rectangles indicate the area from folia III and VI that are shown in higher magnification. Different cerebellar layers are also indicated: WM (white mater), GL (granule cell layer), PC (Purkinje cell layer) and ML (molecular layer). Quantitative data are expressed as means \pm SEM for each group. Results were compared using the Mann–Whitney U -test (GraphPad Prism Software). Significant effects are indicated by asterisks ($*P < 0.05$, $**P < 0.01$, $***P < 0.001$). Scale bars: 1 mm for whole cerebella and 25 μm for magnifications. Rotarod analysis shows that motor coordination decreases less rapidly in the GNP-treated group ($n = 14$) from 12 weeks posttransplantation onward when compared with the control group ($n = 12$). Results were compared using a 2-way ANOVA (GraphPad Prism Software).

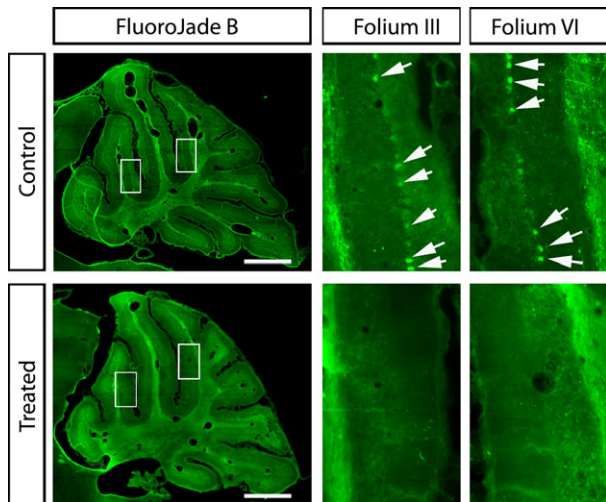


Figure 4. Detection of neurons undergoing degeneration using Fluoro-Jade B. Fluoro-Jade B, a high-affinity fluorescent marker specific for degenerating neurons, allows for the detection of the degenerative process and stains both neurites and cell bodies. Fluoro-Jade B staining of GNP-treated and control Hq cerebella 2 months posttransplantation shows Purkinje cell bodies undergoing degeneration in the control group only (white arrows) Scale bar: 1 mm.

40 rpm over a 5-min period, and the latency to fall recorded weekly for 18 weeks after GNP transplantation. No significant difference was seen during the first 10 weeks of the test.

However, GNP-treated Hq mice performed significantly better than control mice starting 12 weeks post-transplantation (Fig. 3). Interestingly, 7.5-month-old GNP-treated animals (i.e., 18 weeks posttransplantation) performed as well as 6-month-old controls, indicating a slowing of the progression of ataxia. In agreement with the neuronal preservation seen at this age, these data show that GNP transplantation also improved sensorimotor performance.

GNP transplantation is associated with local microgliosis

To determine the fate of the transplanted cells in vivo, we labeled cerebellar sections of a second batch of animals with an anti-human nucleus (AHN) antibody that specifically recognizes the nuclei of human cells, or with the anti-SC121 antibody, which stains the cytoplasm of human cells. One week posttransplantation, human cells were detected in all animals. One month posttransplantation, human cells were still detected in three of six animals, and had migrated locally throughout the injected folia (IV–V) and, to a lesser extent, into adjacent folia (III and VI). Many cells were positively labeled by a human-specific antibody to the progenitor marker nestin. Co-labeling for AHN and doublecortin (DCX), β -III tubulin (TuJ1) or MAP2 revealed that these GNPs were also capable of

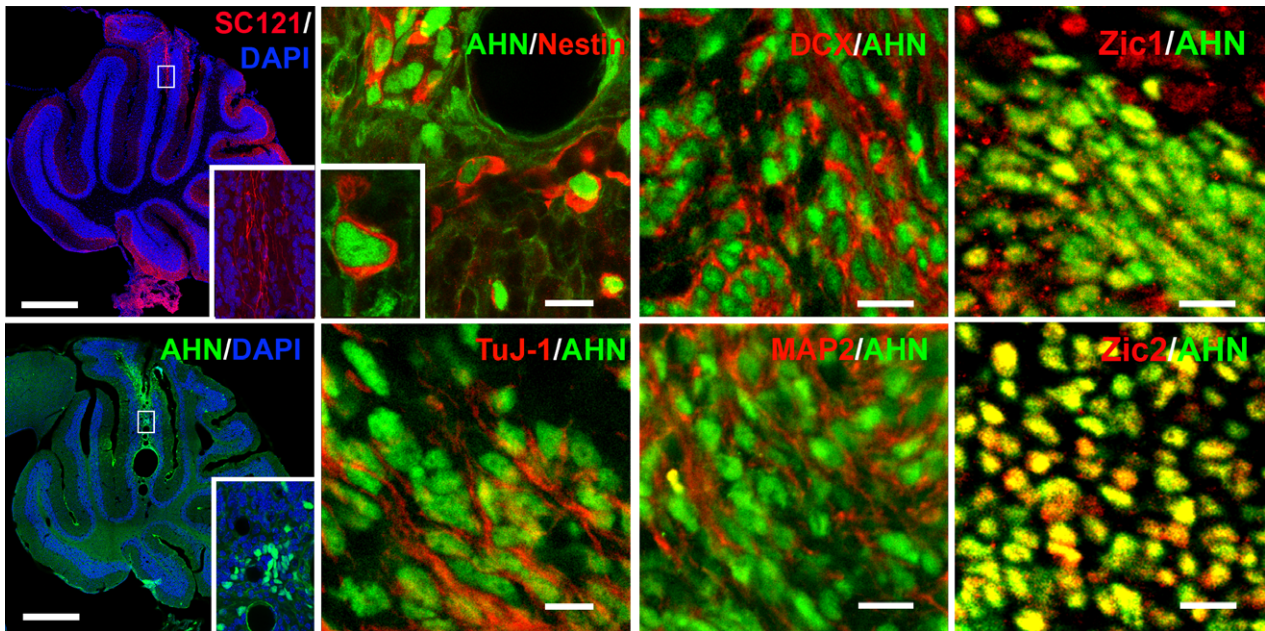


Figure 5. Detection and neuronal differentiation of human GNPs in the cerebellum of Hq mice 1 week and 1 month after transplantation. Immunohistochemistry of GNP-treated Hq cerebella using the human cytoplasmic SC121 antibody indicates that human GNPs survive 1 week after they have been transplanted (first inset). The co-labeling of human GNPs with the anti-human nucleus antibody (AHN) and neuronal antibodies shows that in animals in which GNPs have survived for 1 month posttransplantation (half of the animals), a number of human cells are labeled by antibodies to human nestin (which does not recognize mouse nestin), doublecortin (DCX), TuJ1, MAP2 and the granule cell transcription factors Zic1 and Zic2. Scale bar: 1 mm (whole cerebellum) and 25 μ m (magnifications).

differentiating into neurons (Fig. 5). Co-labeling with AHN and the cell-cycle-dependent antigen Ki67 revealed few proliferative cells (Fig. 6A) and no tumor formation was observed. In contrast, we found few or no human cells in the three other animals, indicating that the GNPs had not survived up to this time point in all cases. At this age, strong microglial activation occurs in the cerebellum of Hq mice.³ Accordingly, Iba1-positive microglia/macrophages were found throughout the cerebellum, and were particularly abundant around the transplanted area (Fig. 6A and B), suggesting that the GNPs had triggered acute local microgliosis. Consistent with this, labeling for the activation-associated macrophage mannose receptor, CD206, was also increased in transplanted cerebella (Fig. 6B). Interestingly, while transplantation of either dead GNPs or human fibroblasts (hFibs) resulted in a similar Iba1 reaction in Hq mice, GNPs did not trigger any detectable microgliosis when transplanted into wild-type animals (Fig. S1). This indicates that the local microgliosis observed is specific to the Hq phenotype in reaction against stranger cells. Moreover, no human cells were detected in GNPs-treated Hq mice beyond 2 months, whereas they were still abundant in wild-type or immunodeficient Nude mice (Fig. S2). This suggests that the strong transplantation-induced microglial reaction had likely led to human cells elimination by this time point.

Endogenous neurogenesis occurs in GNP-transplanted Hq mice

At 2 months posttransplantation (i.e., at 5 months of age), a large number of cells positive for mouse nestin was detected throughout the molecular and granule cell layers in all GNP-treated animals (compared to almost none in controls), predominantly in the injected folia (Fig. 7A), suggesting that human cells had activated endogenous nestin-positive cerebellar progenitors. The same phenomenon was observed following dead GNPs or hFibs transplantation but was not seen in GNP-treated wild-type mice, indicating that this reaction was specific to Hq mice but was not specifically due to GNPs (Fig. S1).

To determine if endogenous neurogenesis could occur in GNP-treated Hq animals, mice were given BrdU injections intraperitoneally every alternate day for 30 days, starting at 5 months, and sacrificed at 7 months (Fig. 7B). Confocal microscopic analysis of the granule cell layer showed several nuclei positive for both BrdU and NeuN, indicating that endogenous neurogenesis had occurred (Fig. 7C). The number of BrdU-positive neurons was significantly higher in folia adjoining the injected folia (Fig. 7D), consistent with nestin labeling at earlier stages. Thus, endogenous neurogenesis occurs in

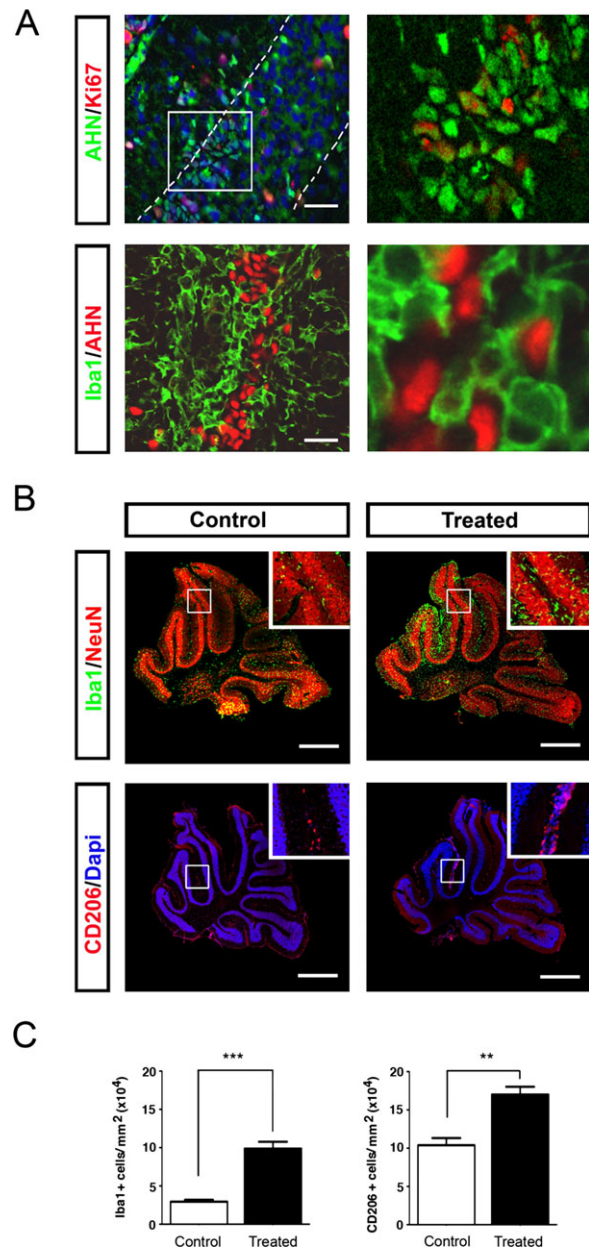


Figure 6. Ki67 labeling of transplanted GNPs at 1 month and reactive microglia at 1 and 2 months posttransplantation. (A) Immunohistochemistry of GNP-transplanted Hq cerebella 1 month posttransplantation shows that human cells express Ki67 only weakly and do not form tumors but are massively surrounded by macrophages-expressing Iba1. Scale bar: 25 μ m. (B) Immunohistochemistry of GNP-transplanted and control Hq cerebella 2 months posttransplantation shows strong immunoreactivity for the macrophage-associated markers Iba1 and CD206 in the GNP-treated group only, indicating that a strong microglial reaction persists in the transplanted area, although human cells are not present anymore. Scale bar: 1 mm. (C) Quantitative data are expressed as means \pm SEM for each group. Results were compared using the Mann-Whitney *U*-test (GraphPad Prism Software). Significant effects are indicated by asterisks (** P < 0.01, *** P < 0.001).

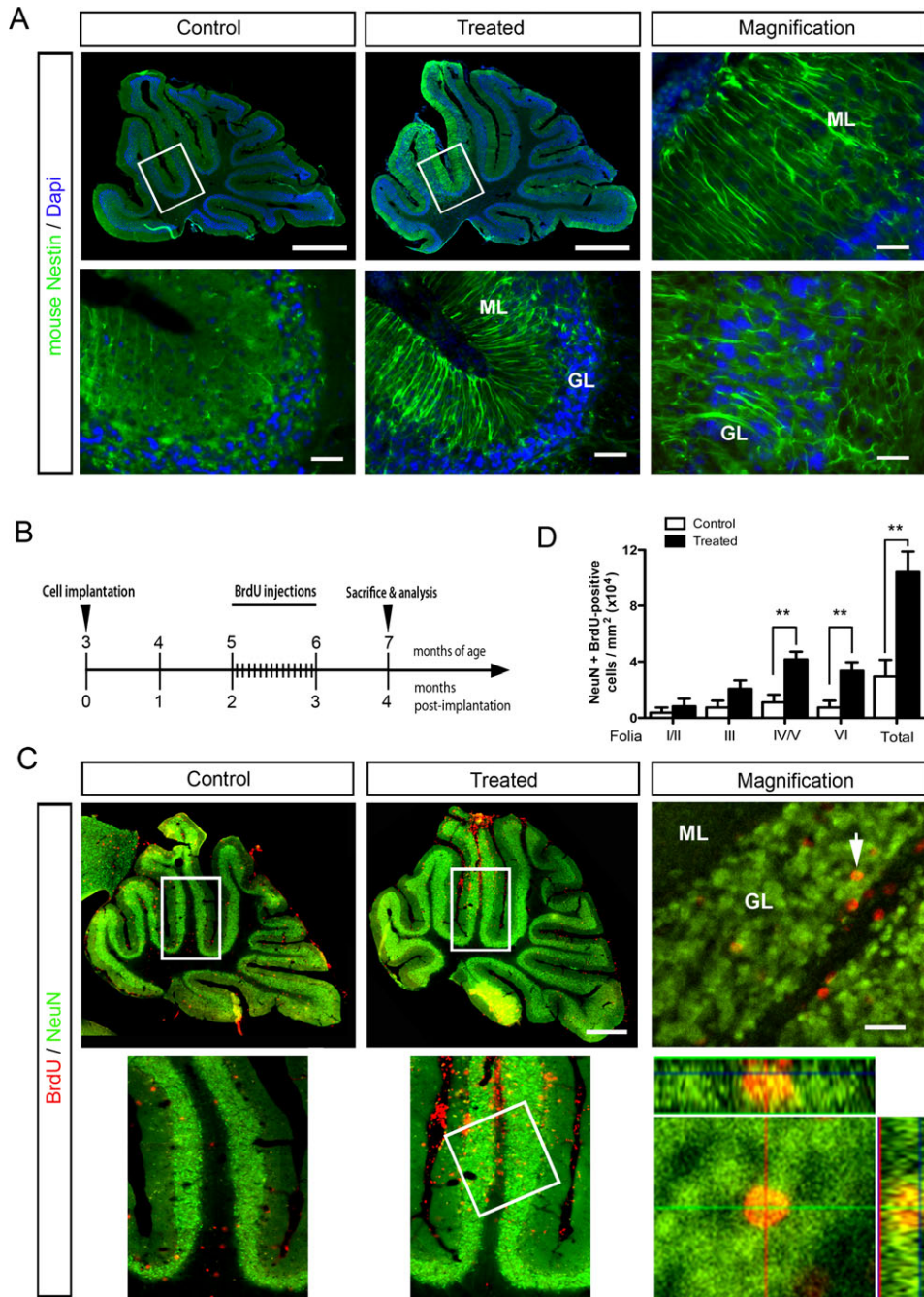


Figure 7. Neural induction and endogenous neurogenesis in GNP-transplanted Hq mice 2 and 4 months after transplantation. (A) Immunohistochemistry of GNP-treated and control Hq cerebella 2 months posttransplantation shows strong labeling with a mouse-specific antibody to the neural marker nestin in the GNP-treated group only. High magnification images of the GNP-treated cerebellum show that nestin-expressing cells are present in the molecular layer (ML) as well as in the granular layer (GL). Scale bars: 1 mm for whole cerebella, 50 μ m for lower panels and 25 μ m for high magnification images (B) Intraperitoneal BrdU injection procedure. GNP-treated Hq animals received BrdU injections every alternate day between 2 and 3 months after transplantation, and were sacrificed 1 month later, that is, 4 months after transplantation. (C) Immunohistochemistry of GNP-treated/BrdU-injected Hq cerebella shows that a number of BrdU-positive cells express the neuronal marker NeuN and are found in the granular layer 4 months after transplantation. Scale bars: 1 mm for whole cerebella, 25 μ m for high magnification. (D) Quantification of NeuN/BrdU-positive cells in different folia from GNP-treated/BrdU-injected Hq mice. Quantitative data are expressed as means \pm SEM for each group. Results were compared using the Mann–Whitney *U* test (GraphPad Prism Software). Significant effects are indicated by asterisks (***P* < 0.01). Scale bar: 25 μ m.

GNP-transplanted mice in the folia close to the transplanted site.

The cerebellar leptomeninges of GNP-transplanted Hq mice contain neural progenitors

To determine the origin of these nestin-positive progenitors, we looked for proliferating cells 2 months posttransplantation. While no Ki67-positive cells were identified in the cerebellum of age-matched wild-type mice, the leptomeninges of all Hq mice, including nonoperated and PBS-injected controls, displayed a number of Ki67-positive cells, which increased significantly in GNP-treated animals (Fig. 8A and B). Moreover, a number of Ki67-positive cells were positive for mouse nestin (Fig. 8B). These data indicate that the cerebellar leptomeninges of Hq mice contain nestin-positive neural progenitors that are actively proliferating, a process potentiated by GNP transplantation.

Since nestin-positive processes stretched radially across the molecular layer in a pattern typical of Bergmann glia, we asked whether these cells displayed other characteristics of this specialized population of cerebellar radial glia. In the mature cerebellum, Bergmann glia expresses the calcium-binding protein S100-beta, whereas during development they express the radial glial marker RC2 in addition to nestin. Surprisingly, the cell bodies of nestin-positive cells were located both at the pial surface and within the molecular layer and were negative for S100-beta, while cell bodies positive for S100-beta, belonging to typical adult Bergmann glia, were located in between the Purkinje cells as expected, and were nestin-negative (Fig. 8C). In keeping with these results, nestin and S100-beta were almost never colocalized in these radial projections. In addition, these putative Bergmann glia were also negative for both the developmental markers RC2 and Sox2 (not shown), suggesting that they correspond to a third type of leptomeningeal Bergmann glia with progenitor potential in adulthood.

The cerebellar leptomeninges of Hq mice are neurogenic in vitro

To confirm in vitro the neurogenic potential of the cerebellar leptomeningeal progenitors identified in Hq mice, we stripped the leptomeninges from the cerebellar surface of 5-month-old wild-type and Hq animals and cultured them in neural stem cell medium in the presence of bFGF for 10 days. Leptomeninges from wild-type animals curled up and adopted an irregular shape after 2–4 days in vitro (DIV2–4), and finally degenerated. In contrast, leptomeninges from Hq mice rapidly formed dense

floating spheres, the edges of which became refractive around DIV9 (Fig. 9). The number of neurospheres generated from GNP-treated Hq mice was systematically higher than from nonoperated Hq mice. At DIV17–20, the neurospheres as well as most of the cells migrating out of them expressed nestin. At a distance from the neurospheres, many cells also expressed MAP2 (Fig. 9). These findings indicate that the cerebellar leptomeninges of Hq mice have neurogenic potential in vitro that can be potentiated by human GNP transplantation, and confirm that this layer is the source of the neural progenitors seen in Hq mice in vivo.

Discussion

In this study, we asked whether human ESC-derived progenitors could survive and replace or protect dying neurons in a clinically relevant context in which microglial activation is high and the degenerative process has already begun. In the Hq mouse, microgliosis starts around 1–2 months of age, long before the first clinical signs of ataxia.³ Our GNPs were thus injected into a strongly inflammatory environment, which could explain the rapid microglial recruitment to the transplantation site and the elimination of transplanted cells within 2 months. A similar rapid loss of transplanted human cells has been observed in the brain of other animal models of neurological disorders, where transplanted cell survival is very low (less than 5%), irrespective of the immunosuppressive strategy⁹ or source of stem cells used.^{10–14} Consistent with this, GNP transplantation into the cerebellum of wild-type animals, where preexisting microgliosis is absent, resulted in prolonged survival, integration and differentiation in our study, a finding confirmed by observations in immunodeficient nude mice (Fig. S2).

Regardless of the loss of transplanted cells, however, we observed significant improvements at both the histological and sensorimotor levels in GNP-treated Hq mice. This suggests that before or during their elimination, GNPs had released factors or triggered processes that were neuroprotective at the local level. This hypothesis is consistent both with our observation that endogenous neuronal loss was less pronounced in the folia adjoining the transplantation site than in more rostral or caudal ones, and with previous reports of the lack of survival of transplanted cells in the brain even though structural or functional rescue had taken place.^{15,16}

Interestingly, however, Hq mice, unlike wild-type adult mice, appeared to possess progenitors capable of differentiating into mature neurons in the cerebellum in vivo. To our knowledge, this is the first time that such a phenomenon has been convincingly shown to occur in the adult rodent cerebellum, although there has been indirect evidence for

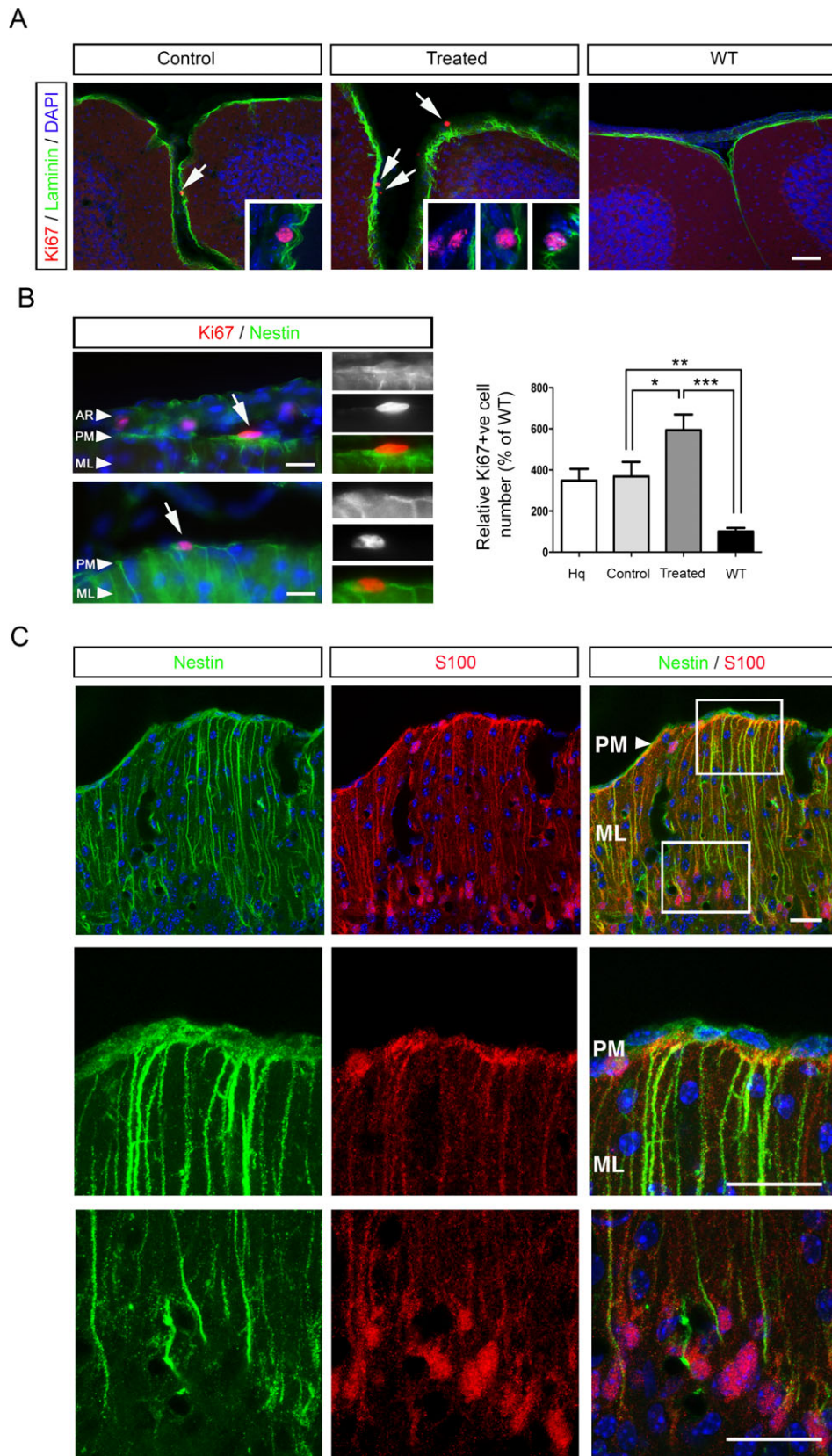


Figure 8. Neural progenitors in GNP-treated Hq mice stem from cerebellar leptomeninges 2 months after transplantation. (A) Immunohistochemistry of Hq cerebella (control and GNP-treated) and WT cerebellum (GNP-treated) 2 months posttransplantation shows the presence of Ki67-positive nuclei at the pial surface of cerebellar folia (white arrows). Scale bar: 50 μm . (B) Co-labeling of Ki67-positive nuclei for mouse nestin shows that some progenitors are still able to proliferate in GNP-treated Hq cerebella (white arrows) and likely stem from the leptomeninges. AR, Arachnoid; PM, Pia mater; ML, molecular layer. Scale bar: 25 μm . Cell counts indicate that GNP-treated Hq animals had more Ki67-positive nuclei than control or nonoperated Hq mice and that the latter two groups had more Ki67-positive nuclei than wild-type animals (WT). Quantitative data are expressed as mean percentages of WT values \pm SEM for each group. Results were compared using a one-way ANOVA (GraphPad Prism Software). Significant effects are indicated by asterisks (* $P < 0.05$, ** $P < 0.01$, *** $P < 0.001$). (C) Immunohistochemistry of GNP-treated Hq cerebella 2 months after transplantation for mouse nestin (green) and the adult Bergmann glial marker S100-beta (red) shows that the two populations, despite their similar morphologies, are distinct (see high magnification insets), and that nestin-positive cells are located either at the pial surface (PM), or in the molecular layer (ML). Scale bar: 25 μm .

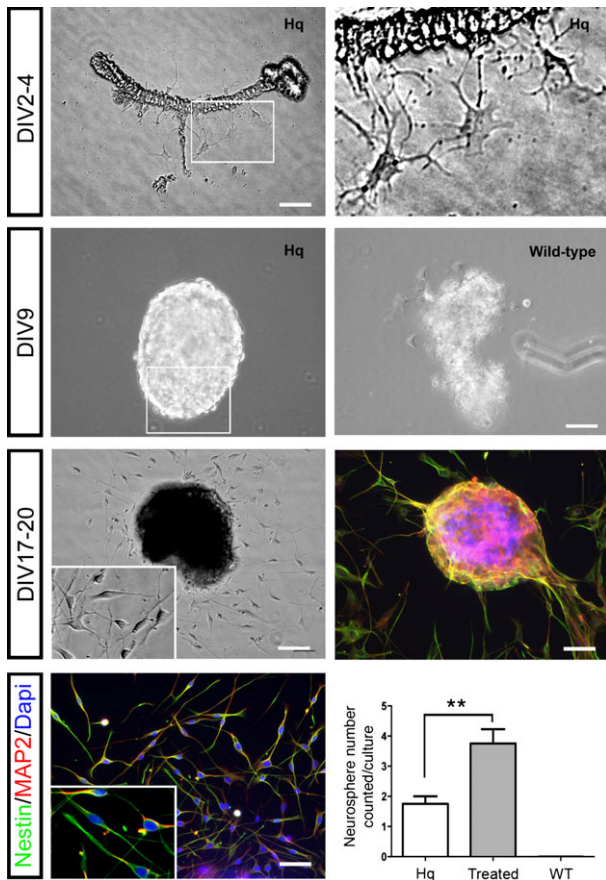


Figure 9. The cerebellar leptomeninges of Hq mice have a neurogenic potential in vitro. Cerebellar leptomeninges from 5-month-old Hq mice ($n = 5$) are able to survive and differentiate in Neurobasal medium in vitro, while those from wild-type animals degenerate ($n = 6$). After several days in culture on Matrigel-coated wells (Day In Vitro DIV17–20), leptomeninges from Hq mice form neurospheres that give rise to neuron-like cells. When dissected from GNP-treated Hq mice ($n = 4$), leptomeninges generate a greater number of neurospheres. Results were compared using a one-way ANOVA (GraphPad Prism Software). Significant effects are indicated by asterisks (** $P < 0.01$). Staining of neurospheres and surrounding cells shows nestin expression. A number of neuron-like cells at a distance from the neurospheres start to express the neuronal marker MAP2 from DIV20. Scale bars: 50 μm , except for immunofluorescence images where they are equivalent to 25 μm .

the existence of multipotent progenitors in the adult cerebellum^{17–19} and new neuronal cells have been reported in the atypical cerebellum of peripubertal rabbits.²⁰

Another unexpected and important finding of our study was that these progenitors were located in the cerebellar leptomeninges, the thin meningeal membranes surrounding the brain and spinal cord, of adult Hq mice, a finding confirmed by the generation of neurospheres capable of differentiating into neurons from these membranes. While the leptomeninges are in direct contact with the nervous tissue, they are not simply protective membranes but have been shown to penetrate neural tissue and contribute to Central Nervous System (CNS) homeostasis by secreting several trophic factors.²¹ Leptomeninges have been recently identified as sites of stem cell recruitment in response to ischemia^{22,23} or brain damage^{21,24,25} suggesting that they also serve as a niche for neural precursors in adulthood during periods of CNS distress. Although these studies focused on specific injuries of the cerebral cortex, they support our observations in the cerebellum of mice undergoing neurodegenerative changes.

The fact that nontreated Hq mice also displayed nestin-positive progenitors and cell proliferation in vivo and neurosphere-generating capacity in vitro is highly interesting, since it suggests that the pathological process might itself trigger the compensatory production of new cells, whether or not these cells succeed in replacing dying neurons. This is the case, for example, in epilepsy,²⁶ Alzheimer's disease,²⁷ Huntington disease,²⁸ and Parkinson disease.²⁹ In addition, the insult to the brain caused by the introduction of exogenous cells may itself augment endogenous neurogenesis, as has been shown for mesenchymal stem cells.^{15,30,31} The pro-neurogenic mechanism of neuronal injury or degeneration could be mediated by inflammatory processes. A growing number of studies show, for example, that acute microglial activation, initially thought to be strictly detrimental to neuronal survival,^{32,33} can influence adult neurogenesis and even exert beneficial neurogenesis-enhancing effects.^{34–37}

Further work is now required to characterize the molecular processes that trigger these unexpected endogenous mechanisms in the adult cerebellum, and to exploit

the neurogenic and neuroprotective potential of these processes in pathological situations.

Acknowledgments

We are grateful to Jane E. Johnson, Southwestern Medical Center, TX, for providing us with the pJ2XnGFP construct, which was modified and used in the construction of the cell line, to Eva Pipiras for assistance with HUES karyotyping and to Cécile Martel for invaluable support. This study was supported by the Institut National pour la Santé et la Recherche Médicale (Inserm), the Centre National de la Recherche Scientifique (CNRS), the Université Paris7, the DHU PROTECT and grants from IFC-PAR/CEFIPRA (projects nos. 3803-3 and 4903-2), the French National Research Agency (project ANR-09-GENO-007), the Princesse Grâce de Monaco Foundation and the Roger de Spoelberch Foundation. M. K. was supported by the Inserm and ANR contract no. ANR-09-GENO-007 to V. E. G.

Conflict of Interest

None declared.

References

- Hersheson J, Haworth A, Houlden H. The inherited ataxias: genetic heterogeneity, mutation databases, and future directions in research and clinical diagnostics. *Hum Mutat* 2012;33:1324–1332.
- Klein JA, Longo-Guess CM, Rossmann MP, et al. The harlequin mouse mutation downregulates apoptosis-inducing factor. *Nature* 2002;419:367–374.
- El Ghouzzi V, Csaba Z, Olivier P, et al. Apoptosis-inducing factor deficiency induces early mitochondrial degeneration in brain followed by progressive multifocal neuropathology. *J Neuropathol Exp Neurol* 2007;66:838–847.
- Lumpkin EA, Collisson T, Parab P, et al. Math1-driven GFP expression in the developing nervous system of transgenic mice. *Gene Expr Patterns* 2003;3:389–395.
- Srivastava R, Kumar M, Peineau S, et al. Conditional induction of Math1 specifies embryonic stem cells to cerebellar granule neuron lineage and promotes differentiation into mature granule neurons. *Stem Cells* 2013;31:652–665.
- Anderson WW, Collingridge GL. The LTP Program: a data acquisition program for on-line analysis of long-term potentiation and other synaptic events. *J Neurosci Methods* 2001;108:71–83.
- Anderson WW, Collingridge GL. Capabilities of the WinLTP data acquisition program extending beyond basic LTP experimental functions. *J Neurosci Methods* 2007;162:346–356.
- Ben-Arie N, Bellen HJ, Armstrong DL, et al. Math1 is essential for genesis of cerebellar granule neurons. *Nature* 1997;390:169–172.
- Jablonska A, Janowski M, Lukomska B. Different methods of immunosuppression do not prolong the survival of human cord blood-derived neural stem cells transplanted into focal brain-injured immunocompetent rats. *Acta Neurobiol Exp* 2013;73:88–101.
- Barker RA, Dunnett SB, Faissner A, Fawcett JW. The time course of loss of dopaminergic neurons and the gliotic reaction surrounding grafts of embryonic mesencephalon to the striatum. *Exp Neurol* 1996;141:79–93.
- Ekdahl CT, Kokaia Z, Lindvall O. Brain inflammation and adult neurogenesis: the dual role of microglia. *Neuroscience* 2009;158:1021–1029.
- Emgard M, Hallin U, Karlsson J, et al. Both apoptosis and necrosis occur early after intracerebral grafting of ventral mesencephalic tissue: a role for protease activation. *J Neurochem* 2003;86:1223–1232.
- Guzman R, Uchida N, Bliss TM, et al. Long-term monitoring of transplanted human neural stem cells in developmental and pathological contexts with MRI. *Proc Natl Acad Sci USA* 2007;104:10211–10216.
- Hicks AU, Lappalainen RS, Narkilahti S, et al. Transplantation of human embryonic stem cell-derived neural precursor cells and enriched environment after cortical stroke in rats: cell survival and functional recovery. *Eur J Neurosci* 2009;29:562–574.
- Munoz JR, Stoutenger BR, Robinson AP, et al. Human stem/progenitor cells from bone marrow promote neurogenesis of endogenous neural stem cells in the hippocampus of mice. *Proc Natl Acad Sci USA* 2005;102:18171–18176.
- Titomanlio L, Bouslama M, Le Verche V, et al. Implanted neurosphere-derived precursors promote recovery after neonatal excitotoxic brain injury. *Stem Cells Dev* 2011;20:865–879.
- Alcock J, Scotting P, Sottile V. Bergmann glia as putative stem cells of the mature cerebellum. *Med Hypotheses* 2007;69:341–345.
- Kamphuis W, Mamber C, Moeton M, et al. GFAP isoforms in adult mouse brain with a focus on neurogenic astrocytes and reactive astrogliosis in mouse models of Alzheimer disease. *PLoS One* 2012;7:e42823.
- Klein C, Butt SJ, Machold RP, et al. Cerebellum- and forebrain-derived stem cells possess intrinsic regional character. *Development* 2005;132:4497–4508.
- Ponti G, Peretto P, Bonfanti L. A subpial, transitory germinal zone forms chains of neuronal precursors in the rabbit cerebellum. *Dev Biol* 2006;294:168–180.
- Decimo I, Fumagalli G, Berton V, et al. Meninges: from protective membrane to stem cell niche. *Am J Stem Cells* 2012;1:92–105.

22. Nakagomi T, Molnar Z, Nakano-Doi A, et al. Ischemia-induced neural stem/progenitor cells in the pia mater following cortical infarction. *Stem Cells Dev* 2011;20:2037–2051.
23. Nakagomi T, Molnar Z, Taguchi A, et al. Leptomeningeal-derived doublecortin-expressing cells in poststroke brain. *Stem Cells Dev* 2012;21:2350–2354.
24. Bifari F, Decimo I, Chiamulera C, et al. Novel stem/progenitor cells with neuronal differentiation potential reside in the leptomeningeal niche. *J Cell Mol Med* 2009;13:3195–3208.
25. Ninomiya S, Esumi S, Ohta K, et al. Amygdala kindling induces nestin expression in the leptomeninges of the neocortex. *Neurosci Res* 2013;75:121–129.
26. Parent JM, Yu TW, Leibowitz RT, et al. Dentate granule cell neurogenesis is increased by seizures and contributes to aberrant network reorganization in the adult rat hippocampus. *J Neurosci* 1997;17:3727–3738.
27. Jin K, Galvan V, Xie L, et al. Enhanced neurogenesis in Alzheimer's disease transgenic (PDGF-APP^{Sw}, Ind) mice. *Proc Natl Acad Sci USA* 2004;101:13363–13367.
28. Curtis MA, Penney EB, Pearson AG, et al. Increased cell proliferation and neurogenesis in the adult human Huntington's disease brain. *Proc Natl Acad Sci USA* 2003;100:9023–9027.
29. Wang S, Okun MS, Suslov O, et al. Neurogenic potential of progenitor cells isolated from postmortem human Parkinsonian brains. *Brain Res* 2012;1464:61–72.
30. Lee H, Kang JE, Lee JK, et al. Bone-marrow-derived mesenchymal stem cells promote proliferation and neuronal differentiation of Niemann-Pick type C mouse neural stem cells by upregulation and secretion of CCL2. *Hum Gene Ther* 2013;24:655–669.
31. Xin H, Li Y, Cui Y, et al. Systemic administration of exosomes released from mesenchymal stromal cells promote functional recovery and neurovascular plasticity after stroke in rats. *J Cereb Blood Flow Metab* 2013;33:1711–1715.
32. Ekdahl CT, Claassen JH, Bonde S, et al. Inflammation is detrimental for neurogenesis in adult brain. *Proc Natl Acad Sci USA* 2003;100:13632–13637.
33. Monje ML, Toda H, Palmer TD. Inflammatory blockade restores adult hippocampal neurogenesis. *Science* 2003;302:1760–1765.
34. Belarbi K, Rosi S. Modulation of adult-born neurons in the inflamed hippocampus. *Front Cell Neurosci* 2013;7:145.
35. Gemma C, Bachstetter AD. The role of microglia in adult hippocampal neurogenesis. *Front Cell Neurosci* 2013;7:229.
36. Nikolakopoulou AM, Dutta R, Chen Z, et al. Activated microglia enhance neurogenesis via trypsinogen secretion. *Proc Natl Acad Sci USA* 2013;110:8714–8719.
37. Ziv Y, Ron N, Butovsky O, et al. Immune cells contribute to the maintenance of neurogenesis and spatial learning abilities in adulthood. *Nat Neurosci* 2006;9:268–275.

Supporting Information

Additional Supporting Information may be found in the online version of this article:

Figure S1. Neural induction and microgliosis reaction in transplanted Hq mice 2 months after transplantation. Immunohistochemistry of cerebellar folia 2 months post-transplantation showing labeling for mouse nestin (upper panel) and the microglia marker Iba1 (lower panel). Strong labeling for nestin is detected in GNP-treated Hq mice, dead GNP-treated Hq mice and in hFib-treated mice but not in PBS-treated Hq mice (control) and GNP-treated Wild-type mice. Similarly, a local microglial reaction is detected in GNP-treated Hq mice, dead GNP-treated Hq mice, and in hFib-treated mice but not in PBS-treated Hq mice (control) and GNP-treated Wild-type mice. Higher magnifications shown correspond to white squares. The different cerebellar layers are labeled: ML, molecular layer; GL, granule cell layer; WM, white mater. Scale bars: 100 μm (lower magnifications) and 50 μm (higher magnifications).

Figure S2. Detection of human GNPs in the cerebellum of wild-type and nude mice 2 months after transplantation. Immunohistochemistry of cerebellar folia of wild-type and nude mice 2 months posttransplantation using either the human cytoplasmic SC121 antibody (left) or doublecortin (DCX, right). Scale bars: 1 mm (whole cerebellum), 100 μm (medium magnification), 25 μm (higher magnification).